Materials Science-Poland, 36(4), 2018, pp. 609-615
http://www.materialsscience.pwr.wroc.pl/
DOI: 10.2478/msp-2018-0079

sciendo

Effect of MgB_2 additives on structure, electrical and thermal properties of $Eu_1Ba_2Cu_3O_7$

NURCAN AKDURAN*

Turkish Atomic Energy Authority, Sarayköy Nuclear Research and Training Center, Saray, Ankara, Turkey

The effect of MgB_2 addition on the $Eu_1Ba_2Cu_3O_7$ (EBCO) ceramics was systematically studied. Series of $Eu_1Ba_2Cu_3O_7$ + x(MgB_2) samples (x = 0 wt.%, 0.05 wt.%, 0.1 wt.%, 1 wt.%, 3 wt.%) were prepared using traditional solid state method. X-ray powder diffraction measurements were used for phase identification. The lattice parameters and orthorombicity decreased with MgB_2 addition. A standard four point measurement method was used to determine transition temperatures T_c of superconducting samples. T_c values of the samples were decreasing with MgB_2 concentration. TGA results indicate thermal stability of doped samples.

Keywords: *rare earth elements, superconductivity, XRD, thermal analysis, electrical resistivity*

1. Introduction

After the discovery of superconductivity in cuprate perovskite compounds [1], a lot of research has been done to investigate the mechanism responsible for superconductivity in these compounds. REBCO type superconductors (RE: rare earth elements) have been effectively examined due to their high potential in electrical and magnetic applications [2–4].

A large number of experimental and theoretical efforts have been made to improve superconductivity and granular coupling of bulk REBCO [5–9]. Chemical doping for high-T_c superconductors has attracted a considerable attention worldwide because it is an effective tool to enhance physical properties of superconductors [30]. This is the most common way to regulate the properties such as the atomic-scale electronic structure, the current carrying capacity and the transition temperature. A lot of studies have been performed on the effect of doping in REBCO system to find the physical mechanism of superconductivity.

The physical properties of high temperature superconductors are very sensitive to deviations from stoichiometry. Some doping elements suppress superconductivity and may disrupt the CuO_2 layer. Studies have confirmed that because of REBCO doping, some microstructural defects, such as point defects, dislocations, twin and grain boundaries are produced in the superconductor. The dopants and defects act as pinning centers, thus, preventing flux movement and increasing the critical current which results in a decrease in critical temperature [10–14]. On the other hand, some studies show that addition of certain materials can enhance the flux pinning behavior and the superconducting transition temperature T_c of REBCO [15]. Increasing of T_c depends on chemical composition, crystallite size, alignment of grains, etc. [16]. The addition of particles in REBCO significantly affects the enhancement of T_c by refining the microstructure, phase formation or increasing hole concentration [17].

The discovery of MgB_2 superconductivity at 39 K in 2001 [38], has generated great interest in basic and applied superconductors research. The compound has the highest T_c among intermetallic superconductors. Soon after, many kinds of elements have been doped into this superconductor in an attempt to advance its superconducting properties [18–20]. However, until now, there has not been any report on MgB_2 addition effects to $Eu_1Ba_2Cu_3O_7$ (EBCO).

*E-mail: akduran@gmail.com

In this work, the effects of addition of MgB_2 on the structural, electrical and thermal properties of EBCO-123 have been examined. By changing the amount of MgB_2 compound, the structural, electrical and thermal properties of doped EBCO materials have been researched.

2. Experimental

The EBCO samples were produced by solid state chemical reaction. The initial powders of Eu_2O_3, $BaCO_3$, and CuO were mixed in nominal stoichiometric ratios according to the chemical formula $Eu_1Ba_2Cu_3O_7$. The starting mixtures were finely ground in an agate mortar for homogenization. In order to eliminate residual carbonates, the samples were calcined in air atmosphere at 965 °C for 48 h. The procedure was repeated typically twice with intermediate grinding. After this process, the samples were synthesized for 48 hours to form $Eu_1Ba_2Cu_3O_7$ at 965 °C and annealed at 500 °C for 36 h in oxygen atmosphere. After annealing, the samples were cooled to room temperature in the turned off furnace. In the second part of the experiment, different weight ratios (x = 0 %, 0.05 %, 0.1 %, 1 % and 3 %) of commercial MgB_2 were added to $E_1Ba_2Cu_3O_7$. EBCO + x(MgB_2) powders were mixed thoroughly using agate mortar and pressed into disc-shaped pellets under a pressure of 10 ton/cm^2. The thickness and the diameter were 0.2 cm and 1 cm, respectively.

The EBCO + x(MgB_2) pellets were sintered at temperatures of 965±5 °C for 24 h in oxygen medium and cooled to 500 °C for 8 h. The sintered samples were annealed at 520 °C in the flowing oxygen for 24 h to provide complete oxygenation. After annealing, the samples were once again cooled to room temperature in the turned off furnace, in oxygen medium.

The structure of the samples was determined by the powder X-ray diffraction technique using CuKα radiation (λ = 1.5406 Å) with a powder X-ray diffractometer. The data were analyzed by least-squares method to calculate unit cell dimensions. The electrical resistivity of the samples was measured by four point resistivity measurements within 77 K to 300 K. Colloidal silver liquid was used as a contact material.

The TGA analysis of the samples was performed with a thermal analyzer at 10 °C/min heating rate under nitrogen flow.

3. Results and discussion

X-ray diffraction patterns of pure and MgB_2 added EBCO samples are shown in Fig. 1. To all diffraction peaks (h k l) values have been assigned. It should be noted that XRD peaks of the samples do not show any peaks of MgB_2 and related compounds. It seems that the dopant MgB_2, added up to 3 wt.%, has not entered the EBCO structure. As a result, XRD patterns of the composite system show no noticeable trace of impurity phases. Most likely, MgB_2 and related peaks with very low intensity may be small compared to the noise level of the background.

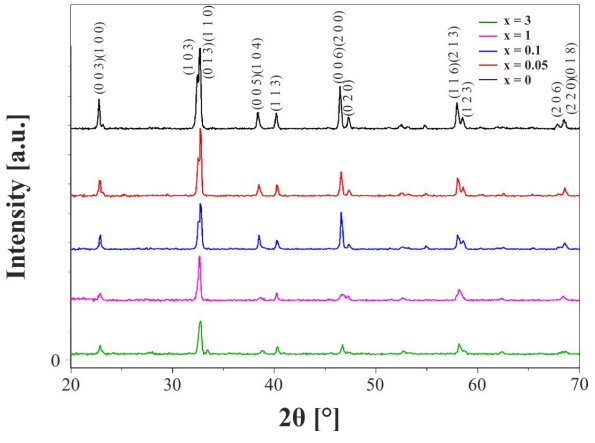

Fig. 1. The XRD patterns of EBCO-$(MgB_2)_x$ system for x = 0 wt.%, 0.05 wt.%, 0.1 wt.%, 1 wt.% and 3 wt.%.

The least-squares refinement method was applied to the determination of lattice parameters. These are in good agreement with the ICDD PDF-2 database. Additionally, with increasing x value for EBCO + x(MgB_2) samples, the lattice parameters of the orthorhombic cell, a and b, approach each other. On the other hand, the increase in concentration of MgB_2, corresponds to a substantial decline of the lattice parameter c. The net result

Table 1. The structural parameters of MgB_2 added EBCO samples.

x [wt.%]	a [Å]	b [Å]	c [Å]	V [Å^3]	η [‰]
0	3.89988	3.8396	11.7109	175.13	15.0
0.05	3.8973	3.8404	11.7009	175.12	15.0
0.1	3.8973	3.8404	11.701	175.12	15.0
1	3.8998	3.8442	11.6847	175.17	14.5
3	3.8661	3.8661	11.6464	174.07	0

is contraction of the orthorhombic unit cell volume. The lattice parameters, volumes and orthorhombic strain values of the samples are presented in Table 1.

The orthorhombic strain $\eta = (b - a)/(b + a)$, is of interest because it is one of important structural quantities. The orthorhombic strain values are given in Table 1. As seen in the table, the strain parameter starts to decrease with the MgB_2 content. The decrease in orthorhombicity indicates the decrease in the orthorhombic strain in the samples. The samples have not remained orthorhombic. These results show that the orthorhombic to tetragonal phase transition took place. The increasing of MgB_2 content resulted in decreasing the strain parameter value to zero.

It is obvious that intensity of the XRD peaks decreases monotonously when MgB_2 concentration is increased and this is clear in Fig. 1 at all diffraction angles. This decreasing in peak intensities is probably associated to the lattice disorder and strain induced in the EBCO lattice due to the doping of MgB_2. Furthermore, the Bragg peak intensity decreased due to increasing of the non-superconducting phase. This means that degradation occurred in orthorhombic phase, while the peak of tetragonal phase was growing [31]. The deterioration in orthorhombic phase is always associated with a change in relative peak intensities at 58.0°, 46.5° and 32.7°, respectively. At the end of the orthorhombic to tetragonal transformation, the two diffraction peaks intensities have been reversed. It is apparent that we can observe much better orthorhombic splitting at 32.7° and 46.5°. This decreasing of the orthorhombic phase resulted in a decrease in the critical temperature T_c.

In Fig. 2, the variation of resistivity as a function of temperature is shown for EBCO – x(MgB_2) system with x = 0 % to 3 %. In Fig. 2a, two different regions are seen for x = 0 %, 0.05 % and 0.1 % samples. These three samples show the expected metallic behavior in the normal state which is one of these regions. The metallic behavior is usually described in terms of electron-phonon interaction. In this region, Baskaran et al. [29] suggested that resistivity can be fitted to $R(T) = A + BT$ functional form. A and B have been obtained from the resistivity slope (dR/dT) and residual resistivity R_{res} at T = 0 K. The other region is characterized by the formation of cooper pairs above the transition temperature [32]. Resistivity deviates from linearity due to the cooper pairs at a characteristic temperature T_s, which indicates the existence of excess conductivity [36].

In Table 2, T_c, T_s, R300 and R_{res} values are given for doped and undoped samples. The room temperature resistivity (R300) greatly depends on grain size, electron scattering effects at grain boundaries and porosity. Its linearity approves the opinion that the preparation and synthesis method was correct. As seen in Table 2, the room temperature resistivity increases with the doping level. This shows expected influence of impurity and doping level of the samples on the room temperature resistivity. Furthermore, at temperatures near absolute zero the electrical resistivity of the samples R_{res} predominantly arises from lattice defects and scattering centers, such as impurities, dislocations, etc. The residual resistivity is often used to express the state of purity of samples. The minimum R300 and R_{res} have been detected for x = 0 % sample. On the other hand, the normal state resistivity, residual resistivity, and temperature of deviation from

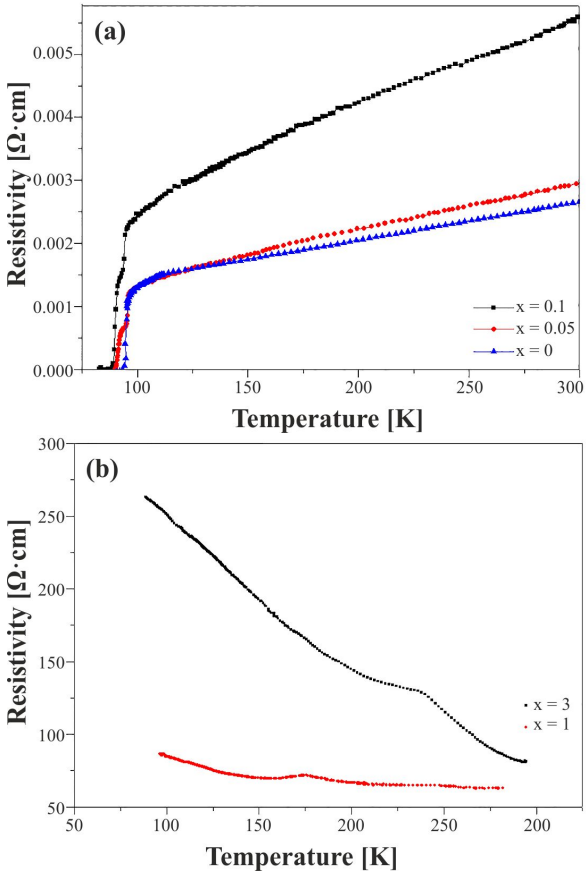

Fig. 2. (a) Temperature dependence of resistivity of EBCO samples for x = 0 wt.%, 0.05 wt.%, 0.1 wt.%; (b) temperature dependence of resistivity of EBCO samples for x = 1 wt.%, 3 wt.%.

linear behavior have been detected for higher values of x. Residual resistivity is of the order of ohms for x = 1 % and 3 %. It means that the MgB_2 additives have affected the superconductivity of the samples. T_s is the temperature of deviation from linear behavior. It is seen that T_s is increasing with the doping level. For x = 1 % and x = 3 %, this deviations is not observed in the samples because of non-metallic behavior. However, a clear increase in the resistivity was observed for these doping levels.

It is clearly seen from the results that T_c values of the samples are decreasing with MgB_2 concentration. This T_c reduction is related to decreasing in grain coupling and enhanced weak-link behavior of polycrystalline samples [21]. It has been known that grain boundaries, misorientation between grains and impurities are detrimental to the transport properties of superconductors. The weak link behavior is generally due to non-superconducting phases, misorientation between adjacent grains, atomic disorder along the boundaries and the presence of impurities [22]. The reduction of transition temperature with the addition of MgB_2 may be caused by reduction in the content of oxygen in CuO chains [23]. It can be related with the mechanism created by disorder in oxygen vacancies [24, 25]. For the cuprate superconductors, the carrier concentration can be improved by apical oxygen movement along CuO_2 planes which is in position between copper oxide plane and chain [33, 34]. These oxygen atoms play a significant role because of acting as hole dopant [28].

According to Zhang et al. [26] there is a universal relationship between hole content and T_c. Examining figure of the relationship in the work [26], T_c/T_{cmax} exhibits a plateau region. After two years, Tallon et al. [27] presented a universal empirical formula between T_c/T_{cmax} and carrier concentration p:

$$T_c/T_{cmax} = 1 - 82.6(p - 0.16)^2 \qquad (1)$$

where p is the hole carrier concentration per Cu ion and it has been determined by this empirical relation. Superconductivity occurs within the limits $0.05 \leqslant p \leqslant 0.27$ which vary slightly in different cuprates. The insulating phase and non-superconducting metallic phase have been observed at $p < 0.05$ and $p > 0.27$, respectively [37]. p values are listed in Table 2. It is found that p values are slightly decreased with doping content.

The observation of different values of T_c and hole concentrations, strongly suggests that presence of MgB_2 affects superconducting grains and significantly suppresses superconductivity. This result is in a perfect agreement with XRD results which were previously described. In addition to this, the broadening of the transition temperature is caused by decreasing oxygen content which is observed in x = 0.05 % and 0.1 % doped samples in Fig. 2a. This widening is also attributed to inhomogeneity of the samples and differences

Table 2. Some electrical parameters for the MgB_2 added EBCO samples.

x [wt.%]	R300 [$\Omega \cdot$cm]	R_{res} [$\Omega \cdot$cm]	T_s [K]	T_c [K]	Hole concentration p [cm^{-3}]
0	2.66×10^{-3}	5.73×10^{-4}	108.6	93.2	0.160
0.05	2.98×10^{-3}	6.78×10^{-4}	120.5	90.7	0.141
0.1	5.56×10^{-3}	12×10^{-4}	120.9	88.0	0.134
1	61.8	–	–	–	–
3	80.1	–	–	–	–

in occupancy by oxygen atoms (O(4) and O(5) sites) [35]. At the high doping level for x = 1 % and 3 %, the normal state resistivity increases and shows a semiconducting behavior as seen in Fig. 2b. The increase in the resistivity can be elucidated by increasing the impurities, defects or by decreasing the relaxation time of electrons as the MgB_2 concentration increases.

In Fig. 3, TGA curves are plotted for x = 0 %, 0.05 %, 0.1 %, 1 % and 3 %. TGA is a technique that measures weight change with respect to temperature. It gives information about changes in physical and chemical properties of materials as a function of increasing temperature. Furthermore, the phase changes may be detected in the temperature range. Critical thermal points (T_1, T_2, T_3 and T_4) are marked by arrows in Fig. 3. As seen in Fig. 3, the crystallization kinetics changes in comparison to the undoped sample. Hydrated oxides decompose with elimination of moisture at low temperatures below 140 °C since the powders were handled in air.

The thermogravimetric curve consists of a two-stage mass loss for x = 0 % and 0.05 %. The first stage corresponds to the temperature region of 400 °C to 900 °C and the other one is above this temperature. For the first zone, the weight loss observed in the curve is connected with oxygen amount that goes out from or into the Cu–O basal plane O(2) and O(5) sites. The increasing temperature at about 400 °C affects mainly this oxygen, which is the most loosely bound in the structure. For this reason, the mass loss in this stage is due to easily released oxygen in the Cu–O chains. At temperature T_2, for x = 0.1 %, 1 % and 3 % a shoulder around 830 °C, corresponding the to melting point of MgB_2 can be seen. The temperature corresponding to the weight loss of 99 % has been labeled as T_3. It is a measure of thermal stability of a material. T_3 shifts to higher temperatures for increased doping level. It should be noted that, x = 3 % sample has the highest thermal stability. This means that removing oxygen from the doped sample is very difficult. Most probably, the oxygen in MgB_2 doped samples is connected with a higher activation energy compared with the undoped sample. T_4 is a final temperature after melting and further decomposition of the samples. In Table 3, it can be seen that the melting point of undoped sample is higher than those of the doped ones.

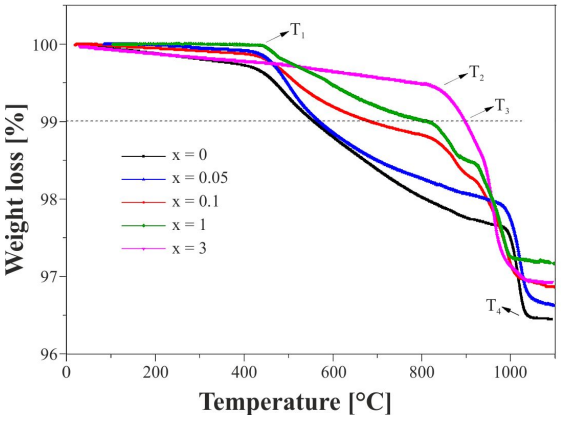

Fig. 3. TGA plots of the MgB_2 added EBCO samples for x = 0 wt.%, 0.05 wt.%, 0.1 wt.%, 1 wt.% and 3 wt.%.

The undoped and doped samples are characterized by different molecular packing and lattice alignment. This is why the melting temperature change is expected. For x = 1 % and 3 % samples, the melting point is the lowest. The results indicate that MgB_2 helps to lower the melting

Table 3. Characteristic temperature values of TGA process for Fig. 3.

x [wt.%]	T_1 [°C]	T_2 [°C]	T_3 [°C]	T_4 [°C]	W_f [%]
0	418	–	552	1039	96.5
0.05	422	–	566	1043	96.7
0.1	424	830	681	1025	97.3
1	449	830	814	1003	97.0
3	–	830	897	997	97.1

temperature of EBCO without producing any other additional compound. The final weight loss W_f for x = 0.1 %, 1 and 3 % is smaller than for other samples because of oxidation susceptibility of MgB_2.

4. Conclusions

In summary, the effect of MgB_2 addition on structure, thermal and electrical properties of the $Eu_1Ba_2Cu_3O_7$ superconductor has been investigated. XRD patterns of EBCO – x(MgB_2) composite system did not show any noticeable impurity peaks. However, the diffraction results revealed that, the orthorhombic structure is not maintained. This result confirms the orthorhombic to tetragonal phase transition. The strain parameter starts to decrease with the MgB_2 content. Increasing of MgB_2 content leads to decreasing the strain parameter value to zero. Lattice parameters of the orthorhombic cell, a and b, approach each other with increasing of doping level. MgB_2 additives affect also transition temperature of the samples, which decreases with MgB_2 concentration. The reduction of T_c with the addition of MgB_2 may be caused by reduction of the content of oxygen in CuO chains.

The thermogravimetric curve consists of a two-stage mass loss for x = 0 % and 0.05 % samples. The first stage corresponds to the temperature region of 400 °C to 900 °C and the second one is above 900 °C. In addition to these zones, for x = 0.1 %, 1 % and 3 % a shoulder can be seen around 830 °C which corresponds to the melting point of MgB_2. The temperatures of a 99 % weight loss shift to higher values with increasing doping level. This means that it is more difficult to remove oxygen from the doped samples. In addition to this, MgB_2 helps to lower the melting temperature of EBCO without producing any other additional compound.

References

[1] BEDNORZ J.G., MULLER K.A., *Z. Physik B*, 64 (1986), 189.

[2] VANDERBEMDEN P., CARDWELL D.A., FREYHARD H.C., VANDERHEYDEN B., *Supercond. Sci. Tech.*, 29 (2016), 060302.

[3] BAGRETS N., CELENTANO G., AUGIERI A., NAST R., WEISS K.P., *IEEE T. Appl. Supercond.*, 26 (2016), 4800404.

[4] WANG L., WANG Q., *J. Supercond. Novel Magn.*, 27 (2014), 1159.

[5] MURAKAMI M., YOO S.I., HIGUCHI T., SAKAI N., WELTZ J., KOSHIZUKA N., TANAKA S., *Jpn. J. Appl. Phys.*, 33 (1994), L715.

[6] BAGRETS N., AUGIERI A., CELENTANO G., TOMASSETTI G., WEISS K., CORTE A., *IEEE T. Appl. Supercond.*, 25 (2015), 6966731.

[7] SCHLESIER K., HUHTINEN H., PATURI P., *Supercond. Sci. Tech.*, 23 (2010), 055010.

[8] OKA T., MIYAZAKI T., OGAWA J., FUKUI S., SATO T., YOKOYAMA K., LANGER M., *Supercond. Sci. Tech.*, 29 (2016), 024003.

[9] IWAKUMA M., HAYASHI H., OKAMOTO H., TOMIOKA A., KONNO M., SAITO T., IIJIMA Y., SUZIKI Y., YOSHIDA S., YAMADA Y., IZUMI T., SHIOHARA Y., *Physica C*, 469 (2009), 1726.

[10] OZAKI T., WU L., ZHANG C., JAROSZYNSKI J., SI W., ZHOU J., ZHU Y., LI Q., *Nat. Commun.*, 7 (2016), 13036.

[11] DEW-HUGHES D., *Low Temp. Phys.*, 27 (2001), 713.

[12] SELVAMANICKAM V., GHARAHCHESHMEH M., XU A., GALSTYAN E., DELGADO L., CANTONI C., *Appl. Phys. Lett.*, 106 (2015), 032601.

[13] CANTONI C., NORTON D.P., KROEGER D.M., PARANTHAMAN M., CHRISTEN D.K., VEREBELYI D., FEENSTRA R., LEE D.F., SPECHT E.D., BOFFA V., PACE S., *Appl. Phys. Lett.*, 74 (1999), 96.

[14] THANH D.T., TRAN N., DUC H., *VNU J. Sci. Math. Phys.*, 29 (2013), 49.

[15] TERZIOGLU C., OZTURK O., BELENLI I., *J. Alloy. Compd.*, 471 (2009), 142.

[16] ARLINA A., HALIM S.A., KECHIK M.M., CHEN S.K., *J. Alloy. Compd*., 645 (2015), 269.
[17] WANG L.M., HSIEH C.H., CHEN C.C., WU J.F., *Chin. J. Phys.*, 43 (2005), 702.
[18] AĞIL H., AKSU E., GENCER A., *J. Supercond. Novel Magn*., 30 (2017), 2735.
[19] LI W., DOU S.X., *Superconductor*, Sciyo, Portugal, 2010.
[20] TAMPIERI A., CELOTTI G., SPRIO S., RINALDI D., BARUCCA G., CACIUFFO R., *Solid State Commun*., 121 (2002), 497.
[21] NKUM R.K., DATARS W.R., *Supercond. Sci. Tech*., 8 (1995), 822.
[22] IANCULESCU A., GARTNER M., DESPAX B., BREY V., LEBY T.H, GAVRILA R., MODREANU M., *Appl. Surf. Sci*., 253 (1996), 344.
[23] ALECU G., *Rom. Rep. Phys.*, 56 (2004), 404.
[24] RAVINDRAN P., VAJEESTON P., VIDYA R., KJEKSHUS A., FJELLVÅG H., *Phys. Rev. B*, 64 (2001), 224509.
[25] TAMPIERI A., CELOTTI G., SPRIO S., RINALDI D., BARUCCA G., CACIUFFO R., *Solid State Commun*., 121 (2002), 497.
[26] ZHANG H., SATO H., *Phys. Rev. Lett*., 70 (1993), 1697.
[27] TALLON J.L, BERNHARD C., SHAKED H., HITTERMAN R.L., JORGENSEN J.D., *Phys. Rev. B*, 51 (1995), 12911.
[28] HAN P.D., CHANG L., PAYNE D.A., *Physica C*, 228 (1994), 129.
[29] BASKARAN G., ZOU Z., ANDERSON P.W., *Solid State Commun*., 63 (1987), 973.
[30] ZHANG Y., WONG C., SHEN J., SZE S., ZHANG B., DONG Y., XU H., YAN Z., LI Y., HU X., LORTZ R., *Sci. Rep.*, 6 (2016), 32963.
[31] JORGENSEN J.D., BENO M.A., HINKS D.G., SODERHOLM L., VOLIN K.J., *Phys. Rev. B*, 36 (1987), 3608.
[32] AKDURAN N., *Radiat. Eff. Defect S.,* 167 (2012), 281.
[33] LUBRITTO C., ROSCISZEWSKI K., OLES A., *J. Phys. Condens. Matter*., 8 (1996), 11053.
[34] LIU Q.Q., JIN C.Q., YU Y., LI F.Y., LIU Z.X., YU R.C., *Int. J. Mod. Phys. B*, 19 (2005), 331.
[35] BRUYNSERAEDE Y., VANACKEN J., WUYTS B., HAESENDONCK C., LOCQUET J.P., SCHULLER I.K., *Phys. Scr*., 29 (1989), 100.
[36] AKDURAN N., *J. Low Temp. Phys*., 168 (2012), 323.
[37] MOURACHKINE A., *Room Temperature Superconductivity*, Cambridge International Science Publishing, Cambridge, 2004.
[38] NAGAMATSU J., NAKAGAWA N., MURANAKA T., ZENITANI Y., *Nature*, 410 (2001), 63.

Received 2017-04-14
Accepted 2018-07-28